Renewable synthesis fuels for a circular economy

A life cycle assessment

Wen, Du; Kuo, Po Chih; Saeidi, Samrand; Özdemir, Faruk; Maréchal, François

DOI
10.1016/j.resconrec.2024.107851

Publication date
2024

Document Version
Final published version

Published in
Resources, Conservation and Recycling

Resources, Conservation & Recycling 211 (2024) 107851

Contents lists available at ScienceDirect

Resources, Conservation & Recycling

journal homepage: www.sciencedirect.com/journal/resources-conservation-and-recycling

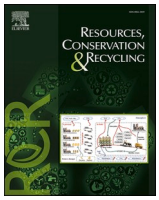

Renewable synthesis fuels for a circular economy: A life cycle assessment

Du Wen [a,*], Po-Chih Kuo [b,*], Samrand Saeidi [c], Faruk Özdemir [d], François Maréchal [a]

[a] Industrial Process and Energy Systems Engineering, Swiss Federal Institute of Technology in Lausanne (EPFL), Rue de l'Industrie 17, Sion 1951, Switzerland
[b] Institute of Industrial Science, University of Tokyo, 4-6-1 Komaba, Meguro-ku, Tokyo 153-8505, Japan
[c] Department of Technologies and Installations for Waste Management, Faculty of Energy and Environmental Engineering, Silesian University of Technology, Konarskiego 18, 44-100 Gliwice, Poland
[d] Process and Energy Department, Delft University of Technology, Leeghwaterstraat 39, 2628 CB Delft, The Netherlands

ARTICLE INFO

Keywords:
Circular economy
Power-to-hydrogen
Biomass-to-hydrogen
Hydrogen storage
Life cycle assessment

ABSTRACT

Renewable synthesis fuels play a crucial role in enabling a circular economy. This study assesses the environmental impacts of power-to-hydrogen and biomass-to-hydrogen routes, considering four hydrogen storage options: hydrogen, ammonia, methane, and methanol with a function unit of 1 liter of a stored hydrogen-derived product. The assessment encompasses metrics such as carbon footprint, use of fossil and nuclear energy, ecosystem quality, human health impact, and water scarcity. The results reveal that the biomass-based route has a lesser impact on global warming potential (GWP), with the system involving chemical looping technology and using ammonia as the storage medium achieving a negative GWP of -7.55 kg CO_2eq. The power-based route outperforms the biomass-based route except for GWP which is influenced by the penetration of renewable energy. Liquid hydrogen is found to be suitable for the fossil fuel-based route, while methane and ammonia are favorable to the power-based and biomass-based routes, respectively.

1. Introduction

Creating a resource-efficient supply chain driven by renewable energy in the chemical and energy sectors is crucial in the circular economy era. Nevertheless, the significant challenge related to the inherent nature of intermittency and fluctuating characteristics of renewable energy sources must be overcome, as this variability can cause instability and system power imbalance in the grid on a large-scale system (Li et al., 2022; Wen and Aziz, 2022). In response to these issues, there has been increasing global attention on power-to-X (P2X) technology, a combination of renewable power and electrochemical conversion devices, aimed at maximizing the utilization of renewable energy sources (Wang et al., 2020; Sorrenti et al., 2022). This technology holds promising potential as a solution to advance the clean energy transition toward a circular economy and sustainability.

Over the last two decades, considerable interest in the development of the P2X process, mainly focused on combining renewable powered-electrolysis and CO_2 hydrogenation, has led to the implementation of several projects worldwide. For example, the Audi e-gas project in Germany, one of the largest industrial power-to-methane (P2M) plants worldwide, successfully demonstrated the production of 1,000 metric tons of synthetic natural gas per year by using CO_2 from biogas and green H_2 obtained from alkaline electrolysis (AE) as sources (Bailera et al., 2017). Since 2013, Haldor Topsøe and other project partners have jointly launched an El-Opgraderet biogas project in Denmark, with the objective of coupling a 40 kWel solid oxide electrolysis cells (SOECs) system with methanation of biogenic CO_2 (Aubin et al., 2023). Moreover, a combination of a 7 kW polymer electrolyte membrane (PEM) electrolyzer and methanation reactors has been demonstrated by the DNV GL, Stedin, and TKI Gas in the Netherlands (Vlap et al., 2015). An overall energy conversion efficiency of 35 % was achieved. Besides, the power-to-ammonia process has also seen significant growth in R&D activity. The latest and the world's first dynamic plant project is under construction and development in Denmark, executed by ABB, Skovgaard Energy, Topsøe, and Vestas (Lindorff, 2023). It is anticipated that the carbon footprint will be reduced by utilizing green ammonia as an alternative to fossil-based agricultural fertilizer.

Concerning the power-to-liquids (P2L) process, numerous projects have so far practiced proof-of-concept trials. In 2014, Sunfire GmbH built the world's first demonstration plant for P2L in Germany to validate the technical concept (Beckman, 2014). The process comprises three steps: (1) green H_2 is generated via SOECs, (2) the reverse water-gas shift reaction is adopted to convert CO_2 and H_2 into syngas, and (3) the syngas is used as inputs for the synthesis of liquid fuels via

* Corresponding authors.
E-mail addresses: du.wen@epfl.ch (D. Wen), pckuo@iis.u-tokyo.ac.jp (P.-C. Kuo).

https://doi.org/10.1016/j.resconrec.2024.107851
Received 15 April 2024; Received in revised form 13 July 2024; Accepted 31 July 2024
Available online 21 August 2024

Fischer-Tropsch (FT) technology. Based on this concept, over three tons of synthetic crude oil were produced (Bioenergy International, 2017). In 2017, Sunfire GmbH announced the construction of an industrial-scale (20MWe) power-to-blue crude plant with an annual capacity of 8000 tons in Norway (Sherrard, 2017). It is noteworthy that a part of the CO_2 source originates from ambient air through direct air CO_2 capture technology. Recently, the Norsk e-Fuel industrial consortium, comprised of Sunfire, Climeworks, Paul Wurth SMS Group, and Valinor, launched a PtL technology project in Norway (Sunfire, 2022; Peters, 2022). The project aims to generate 10 million liters of renewable aviation fuels. Subsequently, it is scheduled to scale up to 100 million liters of jet fuel by 2026. This initiative is expected to reduce approximately 250,000 tons of CO_2 emissions annually (Bioenergy International, 2020).

According to the main demonstration projects reviewed above, it is evident that P2X technology is environmentally attractive and technically achievable for deployment as large-scale renewable energy storage systems. Despite the widely recognized technical feasibility of P2X technologies, to the best of our knowledge, there is scarce research regarding the evaluation of their environmental impact (Zhang et al., 2017; Prabhakaran et al., 2019; Litheko et al.,2023; Lamers et al., 2023; Weyand et al., 2023). Zhang et al. (2017) compared the environmental performance of power-to-hydrogen (P2H) and P2M processes with conventional approaches. It was concluded that the mitigation of greenhouse gas emissions via P2G technology is subject to the origin of CO_2 feedstock and electricity sources. Litheko et al. (2023) evaluated three electrolysis technologies integrated with the P2M process and found out that the magnitude of emissions from highest to lowest was ranked as SOECs, PEM electrolyzer, and AE.

On the other hand, bioenergy (BE) has been recognized as one of the promising renewable energy sources capable of achieving negative carbon emissions when carbon capture, utilization, and storage (CCUS) is simultaneously implemented (Jaspers et al., 2021). Lamers et al. (2023) analyzed the environmental impacts of two P2H technologies (i.e., PEM and SOEC) compared with the steam methane reforming (SMR) route, adopting the United States as a case study. Considering the global warming potential (GWP) indicator, P2H pathways show a significant mitigation trend after 2030, particularly with the incorporation of bioenergy with carbon capture and storage technology. Weyand et al. (2023) investigated the environmental performance of a biomass-based P2L process. It has been shown that biomass processing (i.e., harvesting, handling, and transportation) is one of the most impactful factors on the GWP within the P2L process chain. However, only a few LCA studies consider the storage process of fuels and the integration of CCS technology within the context of the circular economy. This study thus aims to conduct an LCA on the production and storage of renewable synthesis fuels and consider CCS in the system boundary. The biomass-to-hydrogen (B2H) pathway with/without CCUS is also taken into account for comparison.

The predominant methods of green H_2 production, namely P2H, and B2H, in contrast to the fossil fuel-based SMR with and without CCS, are first compared. It is equally imperative to discuss integrating CCS into traditional H_2 production routes, which is considered a transitional solution. Four primary storage methods are used, each dependent on site-specific conditions: liquefaction, storage as ammonia, conversion to methane, and conversion to methanol. The evaluation and comparison of various combinations of H_2 production and storage methods are conducted through scenario analysis to determine the most optimal pathway with minimal negative environmental impacts. A sensitivity analysis is then performed to gain insight into the underlying reasons contributing to high emissions, such as the proportions of solar and wind energy in the renewable mix and the efficiency of carbon capture.

The contributions of this study are as follows:

(i) The establishment of a circular economy framework into current and future energy systems, utilizing hydrogen as both energy storage and carbon storage mediums.
(ii) A comprehensive comparison between P2H and B2H pathways in terms of environmental impact, considering various hydrogen production and storage methods.
(iii) Extend the system boundary to include the storage method with the functional unit rather than limiting the analysis to 1 kg of H_2 production.
(iv) Provision of a reference point with a detailed Life Cycle Inventory (LCI) for future research in the same field, aiding in the advancement of knowledge and understanding.

2. Materials and methods

This study adopts a cradle-to-gate LCA methodology following the guidance outlined in ISO 14040-44 (ISO, 2006a; ISO, 2006b). Sections 2.1-2.3 introduce the first three steps of LCA, namely goal and scope definition, LCI analysis, and life cycle impact assessment (LCIA). Section 2.4 introduces system integration and scenario analysis to tailor the comparison. The final step, interpretation and sensitivity analysis, are presented in Chapter 3.

2.1. Goal and scope definition

The objective of this study is to evaluate the environmental impacts on the production and storage of renewable synthesis fuels within the circular economy framework, as illustrated in Fig. 1. Route (a) serves as the baseline for comparison. The current prevalent method of hydrogen production predominantly involves the utilization of fossil fuels, which needs to be revised to align with the principles of a circular economy due to its reliance on non-renewable resources and its failure to address CO_2 emissions at the production stage.

It is acknowledged that alternative technologies can generate carbon-neutral or even carbon-negative hydrogen. However, integrating these technologies into existing infrastructures is a gradual process and presents various technological and logistical challenges. In the interim, it is crucial to consider transitional solutions that can bridge the gap between current practices and a more sustainable future. One such approach is the integration of carbon capture technologies with existing hydrogen production facilities. By capturing and repurposing the CO_2 emitted during hydrogen production, the environmental impact can be mitigated while gradually transitioning to more sustainable methods.

Indeed, H_2 produced through traditional methods with CCS holds potential for various applications. However, while promising, its use as a fuel within the future energy system presents significant logistical challenges and requires additional time and effort. Typically, fuel production sites are centralized in specific locations, with the produced fuel then being distributed or transported to various smaller, localized areas. The current infrastructure for fuel transportation is primarily designed for methane, and hydrogen requires substantially different handling due to unique properties. Consequently, integrating traditional hydrogen production methods with CCS into the existing energy system can be approached in two ways. First, the liquefaction of hydrogen is a widely acknowledged method for its transportation to energy-demanding locales. Second, both captured CO_2 and hydrogen produced from non-renewable sources can be employed in subsequent processes, such as the production of synthetic fuels like methanol. This approach not only reduces the carbon footprint of hydrogen production in the current energy system but also aligns with the circular economy concept by reusing waste products as resources, thereby closing the loop in the energy production cycle.

Route (b) outlines a P2H-based pathway for the circular economy. The concept revolves around utilizing surplus renewable energy in water electrolysis to produce green hydrogen. This green hydrogen can then be stored through processes such as liquefaction or in representative hydrogen storage carriers like ammonia and methane. Pressure swing adsorption (PSA) and CCS serve as additional suppliers of nitrogen and carbon dioxide feedstocks, respectively. Renewable synthesis

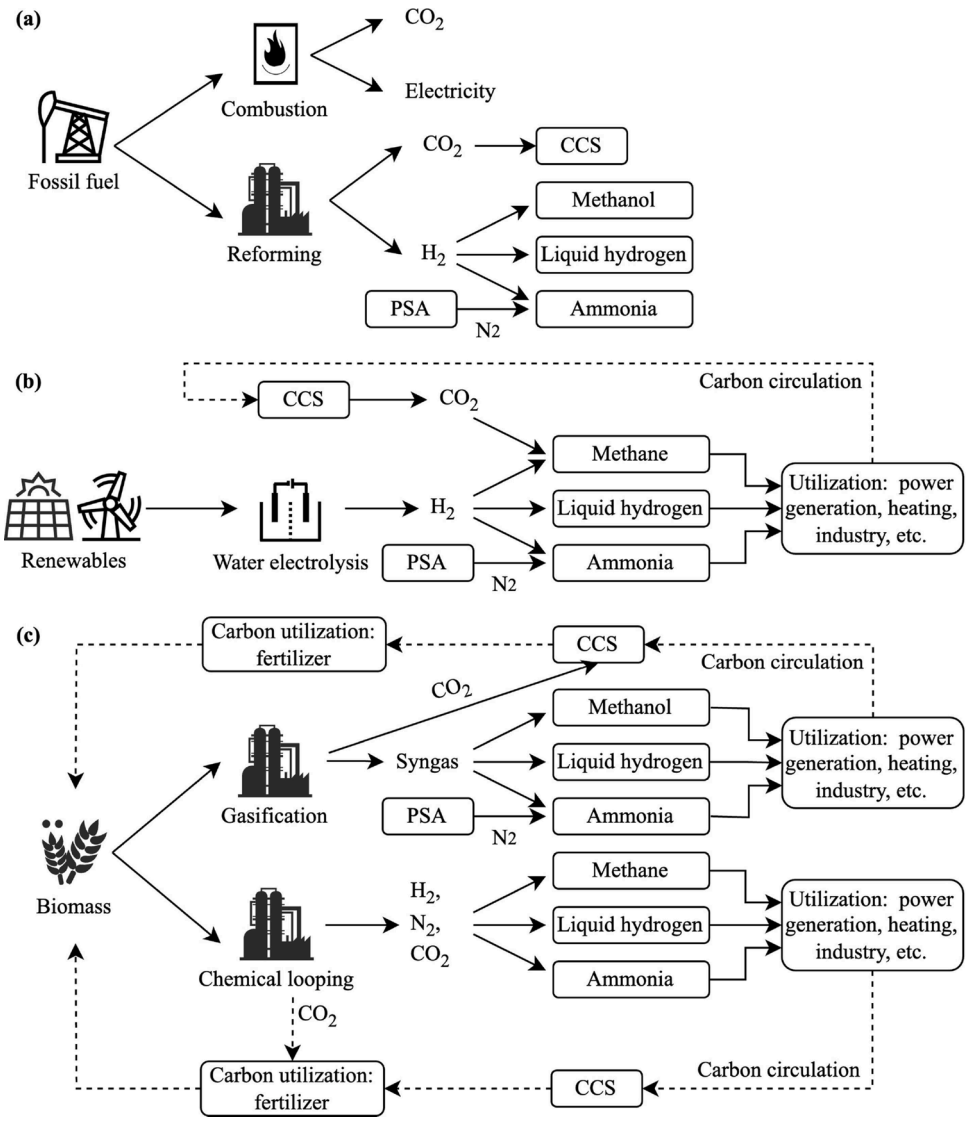

Fig. 1. Schematic of using renewable synthesis fuels for the circular economy, (a) fossil fuel-based, (b) power-based, (c) biomass-based.

fuels can be utilized for power generation to supply electricity and facilitate carbon circulation. It is important to note that this study does not account for other potential applications in the industry and transportation sectors. The surplus electricity, which would otherwise be abandoned, is stored in renewable synthesis fuels and released as needed. Renewable synthesis fuels, such as methane and methanol, can store carbon dioxide as well. After power generation, the emitted carbon dioxide is promptly captured and reintroduced into the production process. Furthermore, integrating waste heat generated during hydrogen production, storage, and power generation processes has the potential to enhance the overall roundtrip efficiency.

Route (c) illustrates a B2H-based pathway for the circular economy. The concept involves generating high-value-added products through the utilization of biomass rather than direct combustion. In this study, straw was used as the representative of biomass. The process entails biomass gasification (GASF), which yields syngas that can be utilized directly to produce methanol. When employing the water gas shift reactor, biomass undergoes conversion into carbon dioxide and hydrogen. This mixture can be readily separated, in contrast to the flue gas resulting from combustion. On the other hand, the chemical looping (CL) process involves the conversion of biomass into carbon dioxide, hydrogen, and nitrogen with the assistance of oxygen carriers. These outputs can be utilized to produce methane and ammonia, which are considered renewable synthesis fuels, given that biomass serves as a carbon-based renewable energy source. The choice between these options of fuel depends on the specific site conditions, available technology, and desired end-products, allowing for flexible and efficient utilization of resources. If the produced syngas contains a higher concentration of CO than CO_2, methanol synthesis is favored. This decision is based on the reaction conditions that facilitate methanol production directly from CO and H_2, thus avoiding the need for additional equipment and reducing overall plant complexity. Conversely, if CO_2 is readily available on-site, both methane and methanol become viable production options.

The system boundaries of the fossil fuel-based (baseline), power-based, and biomass-based routes are depicted in Fig. 2. In this study, the functional unit has been expanded to include 1 liter of a stored hydrogen-derived product in Switzerland in 2024, rather than the commonly used functional unit of 1 kg of hydrogen. This approach is advantageous over the more typical functional unit of 1 kg of hydrogen due to several key factors. First, transporting hydrogen in gaseous form presents significant challenges due to its low density and high compressibility, necessitating complex and costly infrastructure. However, when hydrogen is converted into liquid form, ammonia (Li, 2023), methane (Gholkar, 2021), or methanol (Rolfe, 2022), it becomes denser and easier to handle, store, and transport. Choosing 1 liter of these derivatives or liquefied hydrogen as the functional unit provides a

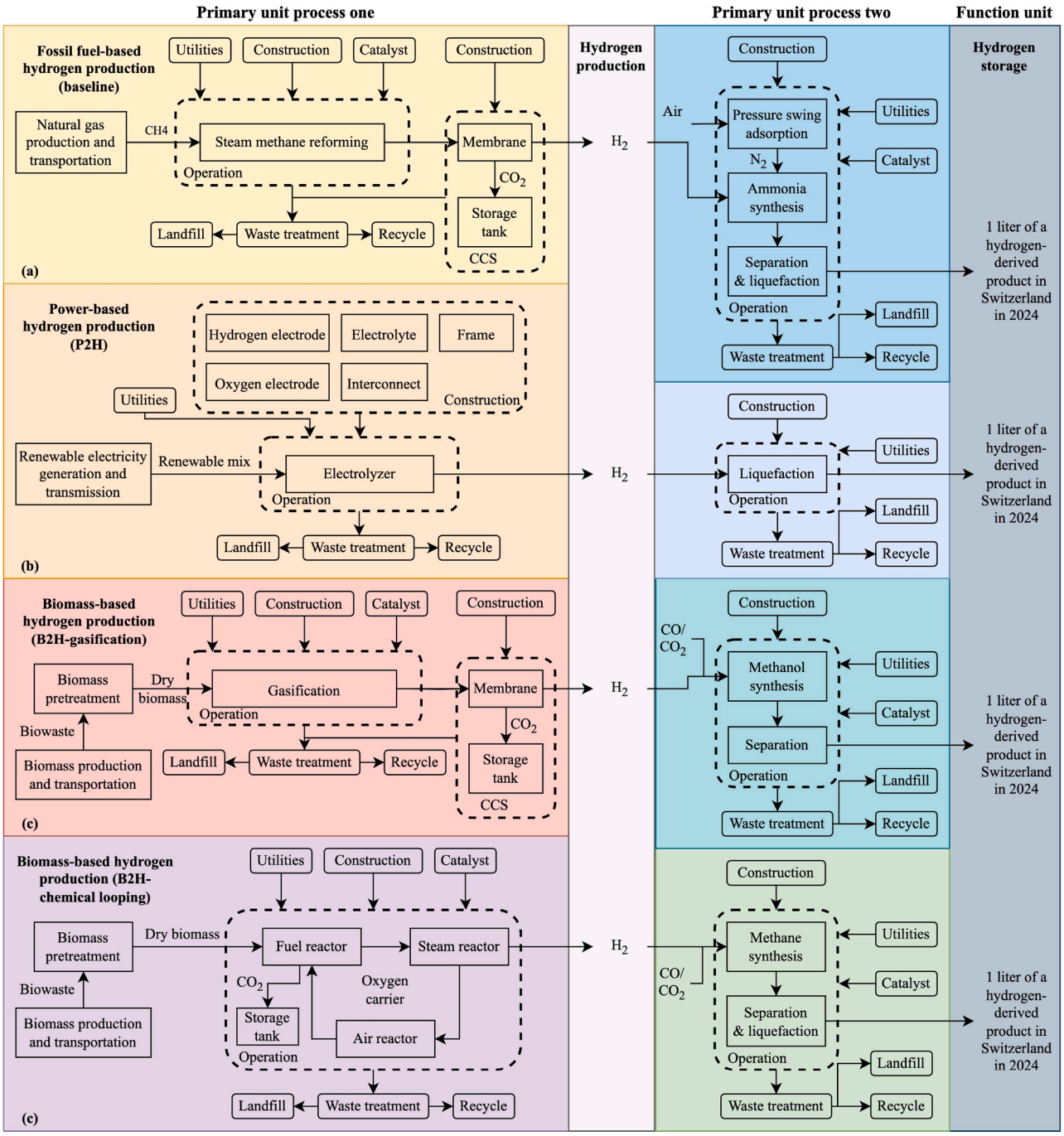

Fig. 2. System boundaries of baseline (a), power-based (b), and biomass-based (c) routes.

practical and effective metric for assessing energy storage and transport efficiencies. This broader perspective enables a more relevant evaluation of distribution systems, supporting decision-makers in optimizing hydrogen logistics from production sites to various usage points.

The study delineates two primary unit processes critical to the production and utilization of hydrogen. The first significant unit process encompasses various hydrogen production technologies, with the intermediate flow from this unit quantified as 1 kg of hydrogen. The process flows of SMR utilized in this study are derived from Susmozas et al. (2013). The graphic illustrates the treatment of natural gas production and transportation as an aggregated process. However, the catalyst is portrayed as a disaggregated process, which is not included in the figure due to spatial constraints. A simple method is employed to disaggregate the construction of the SMR plant, providing an approximate estimation of the materials used, including steel, iron, aluminum, and concrete (Batgi and Dincer, 2024). Regarding waste treatment, two options are available: landfill or recycling. The electrolyzer serves as the primary constituent of the power-based pathway. The process of renewable electricity generation and transmission is commonly regarded as an aggregated process. In contrast to the SMR plant, the construction of the electrolyzer requires more specific consideration of numerous components, such as the hydrogen electrode, oxygen electrode, electrolyte, interconnect, and frame. This is due to the utilization of diverse materials and noble metals in its construction. Fig. 2 does not distinguish between the four types of electrolyzers being studied, namely the Proton Exchange Membrane Electrolyzer (PEMEC), Solid Oxide Electrolyzer (SOEC), Alkaline Electrolyzer (AE), and Anion Exchange Membrane Electrolyzer (AMEC) (Zhao et al., 2020; Gerloff,

2021; Schropp, 2024).

The biomass-based route involves a comparison between two technologies: GASF and CL (Wen and Aziz, 2022). Production and transportation of biomass are considered to be the aggregated process in both cases. After the pretreatment, the dry biomass is directed towards a sequence of reactors wherein oxidation and reduction reactions occur, resulting in the production of hydrogen, carbon dioxide, and nitrogen (in chemical looping). The considerations for utility, catalyst, construction, and waste treatment are similar to those of the fossil fuel-based route. It is important to note that in the CL system, the generation of hydrogen and carbon dioxide occurs in distinct reactors, enabling the accumulation and storage of high concentrations of carbon dioxide. In contrast, the SMR and GASF processes produce a mixture of hydrogen and carbon dioxide as the final product, necessitating the integration of a CCS unit at the end. Following hydrogen production, the second primary unit process involves hydrogen storage technologies. This includes examining different sub-unit processes, such as fuel synthesis and liquefaction. By distinguishing these unit processes, the study systematically evaluates both the production and subsequent handling of hydrogen, ensuring a comprehensive analysis of its lifecycle and implications for energy systems. The general assumptions are outlined below, while the specific assumptions for each technology are provided in **Appendix A**:

(1) the aggregated processes of biomass (straw), materials, electricity, and heating are from the market;
(2) the LCI data for each technology are simplified using the identical approach. The construction of the system only considers the materials used, and maintenance is omitted. Waste is disposed of either in a landfill or through recycling, with the proportion of recycling depending on the materials and remaining constant;
(3) The LCI data of technologies have different input and output conditions, especially in terms of temperature and pressure. Devices used to connect hydrogen production and storage processes and to unify these conditions, such as heaters, compressors, etc., are neglected in the LCA.

Except for assumptions and simplifications, the limitations are mostly due to data availability and quality:

(1) the desired LCI data require extraction from a single source or integration from several sources. Due to the unclear description of the system in references, there is a possibility of missing or double-counting data. Different assumptions and considerations of details can also generate discrepancies in the final results;
(2) maintaining data consistency is difficult. Some references provide industrial data, while others obtain data through process simulation or experiments;
(3) compositions of biomass vary greatly according to types and places, which affects the generality of the results;
(4) technologies are not completely discussed; for instance, only membranes are considered in the CCS system;
(5) transportation from the market to the plant and potential storage leakage are omitted in the analysis.

2.2. Life cycle inventory (LCI) analysis

Information from literature and databases forms the basis for the environmental impact assessment of three routes. Consolidating all the necessary data into a single source poses a challenge. Background processes such as natural gas extraction, renewable electricity generation, and biomass production, including their associated transportation and transmission, are treated as aggregated processes. The ecoinvent 3.6 database provides data for these processes. The foreground processes, including water electrolysis, natural gas reforming, biomass gasification, and chemical looping, among others, are considered disaggregated processes. Initially, data is gathered from real-world cases. In instances where primary data is unavailable or incomplete, alternative sources such as literature are explored, and the data is normalized to fit the same function unit. Additionally, if necessary, data may be calculated based on process simulations. The comprehensive LCI data for each technology is provided in **Appendix A**, where **Table A1** presents the LCI data of SMR, **Tables A2-A5** show the LCI data of four types of electrolyzer, **Tables A6** and **A7** depict the LCI data of biomass gasification and chemical looping, respectively, **Tables A8-A10** give the LCI data of methanol, methane, and ammonia synthesis, and **Table A11** presents the LCI data of membrane. These outputs are generated utilizing OpenLCA 2.0 in conjunction with the ecoinvent 3.6 database.

2.3. Life cycle impact assessment (LCIA)

The LCIA is conducted using the IMPACT World+ v2.0 method, encompassing various mid-point categories such as climate change, fossil and nuclear energy use, freshwater acidification, freshwater ecotoxicity, freshwater eutrophication, human toxicity, ionizing radiations, land occupation, land transportation, marine eutrophication, mineral resources use, ozone layer depletion, particulate matter formation, photochemical oxidant formation, terrestrial acidification, water scarcity. The mid-point categories are summarized into five impacts of carbon footprint: fossil and nuclear energy use (FNEU), remaining ecosystem quality damage (REQD), remaining human health damage (RHHD), and water scarcity footprint (WSF). It is worth mentioning that the Intergovernmental Panel on Climate Change (IPCC) method is employed to compute global warming potential (GWP), which replaces the carbon footprint metric.

2.4. System integration and scenario analysis

An overview of scenarios for the circular economy is shown in

Table 1
Descriptions of scenarios[a] for the circular economy.

Name	Input	Hydrogen production	Carbon capture[b]	Hydrogen storage[c]
A0	Methane	Steam reforming	Without	Liquefaction
A1	Methane	Steam reforming	With	Liquefaction
A2	Methane	Steam reforming	With	PSA+NH_3
A3	Methane	Steam reforming	With	CH_3OH[d]
B1x	Renewables	Electrolysis[e]	Without	Liquefaction
B2x	Renewables	Electrolysis	Without	PSA+NH_3
B3x	Renewables	Electrolysis	With	CH_4
C1	Biomass	Gasification	With	Liquefaction
C2	Biomass	Gasification	With	PSA+NH_3
C3	Biomass	Gasification	With	CH_3OH[d]
C4	Biomass	Chemical looping[f]	Without	Liquefaction
C5	Biomass	Chemical looping	Without	NH_3
C6	Biomass	Chemical looping	Without	CH_4

[a] Scenario A0 serves as the baseline, utilizing fossil fuels without carbon capture. Scenarios B1–3 represent the P2H pathway, while Scenarios C1–6 represent the B2H pathway.
[b] Only membrane-based carbon capture methods are considered in the analysis.
[c] Various hydrogen storage methods are examined, including hydrogen liquefaction, as well as the utilization of ammonia, methane, and methanol as hydrogen storage mediums.
[d] In methanol synthesis, syngas composed of H_2 and CO serve as the primary feedstock. The syngas produced by reforming and gasification processes are directly utilized, eliminating the need for a water gas shift reactor.
[e] Four types of water electrolysis technologies are evaluated, namely SOEC, PEMEC, AE, and AMEC. They are distinguished by subscripts, such as B11, B12, B13, and B14, respectively.
[f] In the chemical looping technology, the resulting gases in the three reactors are CO_2, H_2, and N_2, which serve as feedstocks for ammonia and methane synthesis. Therefore, there is no need to install CCS and PSA units.

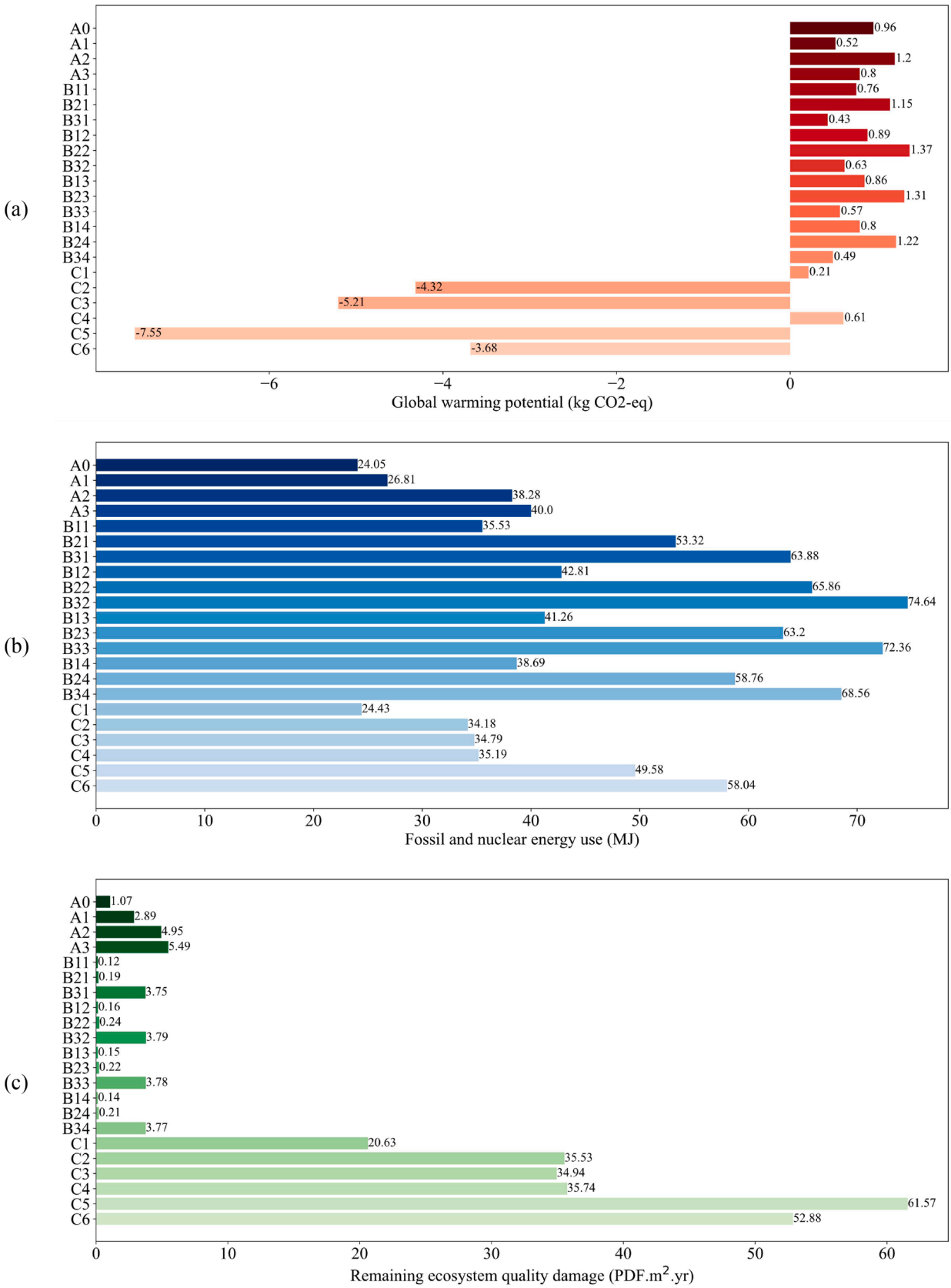

Fig. 3. LCIA results of (a) global warming potential, (b) fossil and nuclear energy use, (c) remaining ecosystem quality damage, (d) remaining human health damage, and (e) water scarcity footprint.

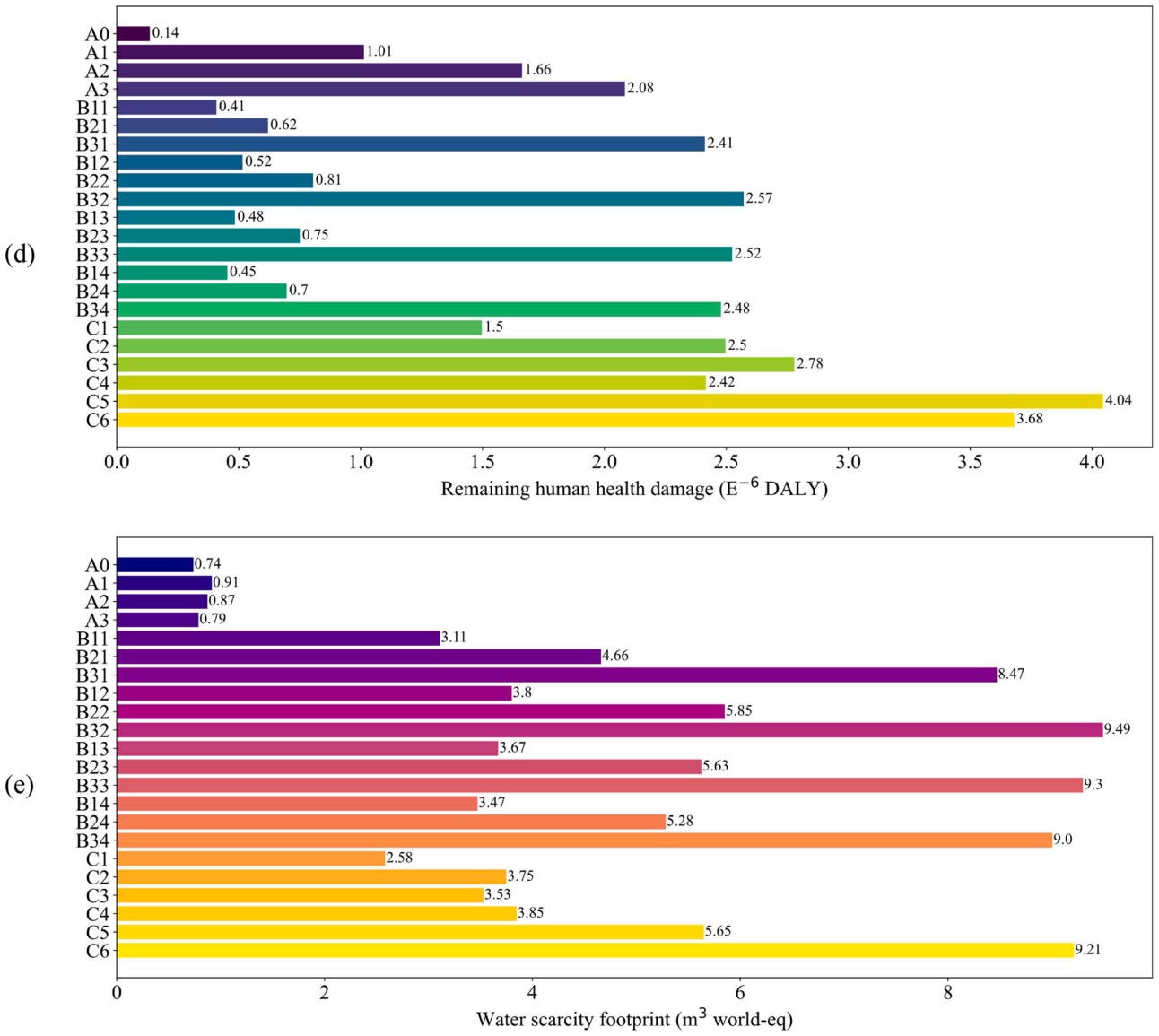

Fig. 3. (*continued*).

Table 1. Fossil fuel, power, and biomass-based routes are evaluated and compared, denoted by A, B, and C, respectively. Methane has been selected as the representative fossil fuel due to its significant contribution, accounting for approximately 50 % of hydrogen production derived from fossil fuels. Coal gasification and oil reforming are excluded from the analysis for the sake of simplicity. The analysis initially relies on electricity from the market, followed by a transition to a renewable energy mix, primarily comprising solar and wind energy. The proportion of solar and wind energy within this mix plays a crucial role in shaping the environmental impact, a factor explored in detail through the sensitivity analysis. Route B involves the consideration and comparison of four types of electrolyzers, which are not included in the table. Besides, there has been limited research on the environmental impact of AMEC compared to the other three commonly used electrolyzers (SOEC, PEMEC, and AE). It is competitive due to its low cost, high efficiency, and high durability.

Route C involves the utilization of GASF and CL. CL is an emerging technique currently in the pilot scale. It is characterized by high carbon capture potential, as carbon dioxide can be enriched and captured in the fuel reactor without additional separation steps. This characteristic holds significant promise for reducing carbon emissions in the production process. It should be noted that the selection of biomass is contingent upon the available LCI data. This research does not delve into the influence of various types of biomass on the final results. In scenarios using methanol as the final product, syngas is directly sent to the methanol synthesis without the inclusion of the water gas shift reactor and CCS unit. However, in other scenarios where methane synthesis is involved, a CCS unit is used to capture carbon dioxide from the output mixture gas or to provide the feedstock for methane synthesis. In each route, liquid hydrogen and ammonia are considered as the hydrogen storage methods. The choice between methane and methanol depends on the byproduct, taking into account the utilization of carbon. If the byproduct is carbon dioxide, it will be stored in methane. Conversely, if the byproduct is carbon monoxide, syngas can be used to produce methanol.

3. Results and discussion

The LCA of 22 scenarios for the circular economy has been conducted, encompassing the evaluation of GWP, FNEU, REQD, RHHD, and WSF. The breakdown of impacts elucidates the contribution of each process. Additionally, a sensitivity analysis delineates the trend concerning varying proportions of the renewable energy mix and efficiencies of carbon capture.

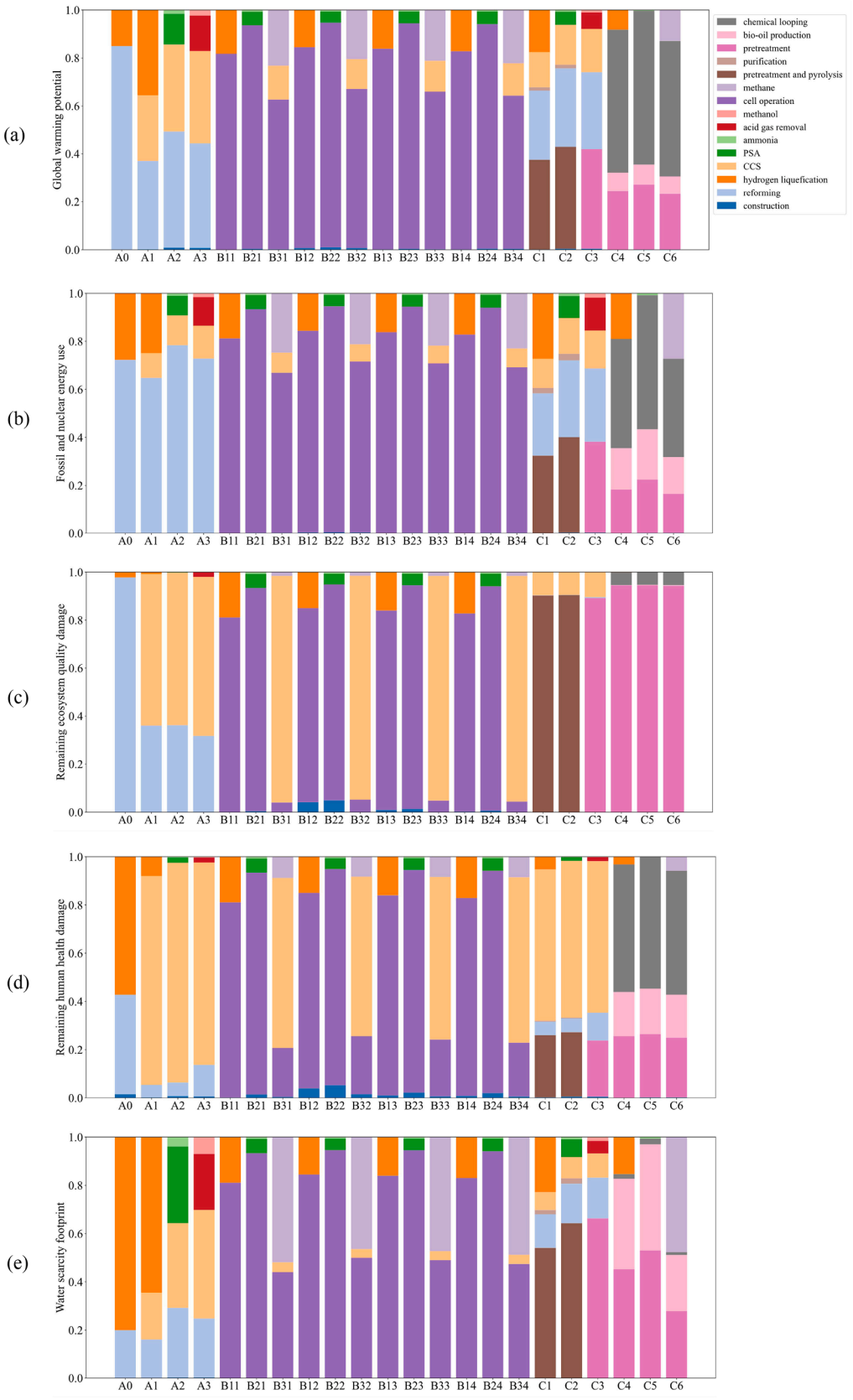

Fig. 4. Breakdown of global warming potential (a), fossil and nuclear energy use (b), remaining ecosystem quality damage (c), remaining human health damage (d), and water scarcity footprint (e).

3.1. LCIA results

Figs. 3 and 4 display the LCIA results for five impacts and their corresponding breakdowns, respectively. The comprehensive results can be found in **Appendix B**. Fig. 3**(a)** illustrates the GWP across 22 scenarios. Scenario A0, which is the baseline with SMR for hydrogen production, liquefaction for storage, and no carbon capture unit, yields 0.96 kg CO_{2eq} per liter of liquid hydrogen. If the carbon capture technology with an efficiency of 90% is considered, the GWP decreases to 0.52 kg CO_{2eq}, as shown by Scenario A1. Considering the storage density of liquid hydrogen, ammonia, and methanol, the GWP varies accordingly, where using ammonia as the storage under this situation has the highest emission of 1.2 kg CO_{2eq} per liter of liquid ammonia, followed by methanol and liquid hydrogen.

When it comes to power-based route B, no matter which P2H technology it uses, the GWP is generally higher than that of fossil fuel-based route A in most instances. It is attributed to the electricity supply as it is the major part of the GWP for the power-based route B, as illustrated in Fig. 4**(a)**. For a fair comparison, the electricity utilized in each scenario comes from the same source of the electricity market. However, since the Swiss electricity grid does not exclusively rely on renewable energy sources, the emissions associated with electricity usage may exceed initial expectations. The choice of P2H technology has less influence on the GWP; for instance, the GWPs of B11-SOEC, B14-AMEC, B13-AE, and B12-PEMEC, in ascending order, are 0.76, 0.8, 0.86, and 0.89 kg CO_{2eq} per liter of liquid hydrogen, respectively. **Tables A2-A5** offer insights into the electricity consumption for operation, revealing that SOEC exhibits the highest efficiency, whereas PEMEC has the lowest efficiency. Although the storage density of liquid methane is six times higher than that of liquid hydrogen, the integration of CCS makes it a suitable storage method for the power-based route with less environmental impact. It ranges from 0.43 to 0.63 kg CO_{2eq}, which results in a reduction of around 60% in GWP compared to the highest GWP when ammonia is used. Based on the current energy structure, only when the cell efficiency is higher than a threshold, such as SOEC, in the power-based route, B21, using ammonia as the storage medium, can beat the competitor of A2 in the fossil fuel-based route. B21 and A2 have GWPs of 1.15 and 1.2 kg CO_{2eq}, respectively.

The biomass-based route C exhibits the lowest GWP. The negative value signifies a positive environmental benefit. Carbon emissions associated with the construction and operation of systems in route C can be mitigated through carbon capture processes. It is noteworthy that the carbon dioxide emitted from biomass originates from the environment. Therefore, in calculating the GWP, it is necessary to subtract the amount of captured carbon dioxide from the total emissions. The details of carbon emission, captured carbon dioxide, and emitted carbon dioxide can be found in **Appendix B**. The biomass CL technology can fix 16.7 kg of carbon dioxide per kg of hydrogen, whereas the biomass GASF technology generates 9 kg of carbon dioxide per kg of hydrogen, which is fixed by a CCS unit, as demonstrated in **Tables A6** and **A7**. It should be noted that in both cases, a carbon capture efficiency of 90 % is considered. When using the same storage medium of ammonia, the GWP of scenario C5 is -7.55 kg CO_{2eq}, while it is -4.23 kg CO_{2eq} in scenario C2, which presents the carbon capture capability of CL. However, without the deduction of captured carbon dioxide, the GWP of CL is higher than that of GASF. Since the carbon capture unit is integrated into the B2H process, the captured carbon dioxide will be scaled up when considering the storage process. The scaling factor is correlated to the density, where liquid hydrogen is the lowest, followed by methane, ammonia, and methanol. That explains why scenarios C1 and C3 have positive GWPs of 0.21 and 0.61 kg CO_{2eq}, respectively.

Fig. 3**(b)** illustrates the FNEU across 22 scenarios. The baseline scenario A0 utilizes 24.05 MJ of fossil and nuclear energy, primarily consumed by the reforming process, which utilizes natural gas as feedstock and heating. After integrating CCS, scenario A1 entails an additional 2.76 MJ of energy consumption, mostly from the fabrication of the membrane and operation of the system. Compared to scenario A1, different storage densities and extra equipment make scenarios A2 and A3 have more energy consumption, which is 38.28 and 40 MJ, respectively. In route B, regardless of the type of water electrolysis technologies employed, energy consumption is highest among the three routes due to the substantial electricity usage during operation. The difference is presented in efficiency, which is the same as that of GWP. Consequently, it maintains the same ranking as observed in GWP. Specifically, B11-SOEC, B14-AMEC, B13-AE, and B12-PEMEC exhibit FNEUs of 35.53 MJ, 38.96 MJ, 41.26 MJ, and 42.81 MJ, respectively. The utilization of ammonia and methane as hydrogen storage mediums necessitates approximately 50% and 80% increases in FNEU, respectively. In route C, scenarios using biomass GASF technology have the lowest FNEU among the three routes. It is attributed to the absence of natural gas feedstock compared to route A and lower electricity consumption than route B. However, the lowest FNEU of 24.43 MJ in scenario C1 is still higher than that of the baseline scenario A0, which is due to the extra CCS system. The adoption of CL necessitates a higher heat duty, positioning its energy consumption between routes A and B.

Fig. 3**(c)** illustrates the REQD across 22 scenarios. The baseline scenario A0 demonstrates a relatively low value of 1.07 PDF·m^2·yr. This primarily originates from the wastes and emissions generated during operation. The increase in REQD in other scenarios within route A is primarily attributed to the utilization of the CCS unit, which accounts for approximately 70 % of the total increment. Scenarios A1–3 exhibit REQD values of 2.89 PDF·m^2·yr, 4.95 PDF·m^2·yr, and 5.49 PDF·m^2·yr, respectively. The difference in values is attributed to the scaling factor associated with the use of different storage mediums. Route B generally exhibits the lowest REQD, which is less than 0.25 PDF·m^2·yr, except for scenarios B31–33, which integrates a CCS system unit. The use of membranes for carbon capture generates an extra 3.5 PDF·m^2·yr, which is prominent. In route C, REQD values are several orders of magnitude larger than those of routes A and B, increasing to 20–60 PDF·m^2·yr. This disparity primarily arises from the utilization of biomass, which accounts for over 90% of the breakdown, as depicted in Fig. 4**(c)**.

Fig. 3**(d)** displays the RHHD across 22 scenarios, with the baseline scenario A0 exhibiting a relatively low value of 0.14E-6 Disability-adjusted life year (DALY). Similar to the trend observed in REQD, the utilization of the CCS unit exerts a significant influence, resulting in RHHD values in scenarios A1–3 being 10 times larger than that in scenario A0. The contribution of the CCS unit can exceed 80 %, as shown in Fig. 4**(d)**. In route B, without integrating a CCS unit, scenarios have RHHDs ranging from 0.41E-6 DALY to 0.81E-6 DALY. Electricity supply is the major contributor. When integrating the CCS units, scenarios B31–34 have a 5–6 times increase in RHHD, up to around 2.5 81E-6 DALY. The B2H-based route C exhibits the highest RHHD due to the extensive utilization of biomass and the associated emissions and wastes during operation, as detailed in **Tables A6** and **A7**. The highest RHHD of 4.04E-6 DALY comes from scenario C5, which uses CL and ammonia. The disparity observed in using different storage methods primarily stems from differences in scaling factors rather than the inherent characteristics of the process itself.

Fig. 3**(e)** depicts the WSF across 22 scenarios. Route A demonstrates a relatively lower WSF impact, approximately around 0.85 m^3 world-eq, while Routes B and C exhibit a higher WSF impact. The highest WSF achieves 9.49 m^3 world-eq in scenario B32, where water is primarily utilized in water electrolysis and methanation processes. The influence of different electrolyzers is not significant, which is less than 1 m^3 world-eq when using the same storage medium. In contrast, utilizing liquid hydrogen, ammonia, and methane as storage mediums in Route B has a significant difference, which are approximately 3.11 m^3 world-eq (B11), 4.66 m^3 world-eq (B21), and 8.47 m^3 world-eq (B31), respectively. In route C, scenarios C4–6 exhibit a comparable level of WSF compared to that of route B. The primary contribution stems from biomass production and the utilization of process water.

To sum up, scenarios in fossil fuel-based route A have advantages in

RHHD and WSF. Scenarios in power-based route B are promising in REQD and will be beneficial in FNEU if the penetration of renewable energy increases. Because of the biogenic carbon dioxide, biomass-based route C presents carbon negative in most scenarios. Although membrane-based carbon capture technology has an improvement on GWP, it has a negative effect on the other four impacts. The choice of electrolyzers has less impact on LCIA results, which are related to the efficiency, hence SOEC performs well among others. In biomass-based route C, CL outperforms GASF in terms of GWP, while GASF has advantages on other impacts.

Additionally, this study analyzes optimal storage formats across three distinct hydrogen production routes: fossil fuel-based, electrolyzer-based, and biomass-based. For fossil fuel-based hydrogen production, liquefied hydrogen is identified as the most efficient method for reducing CO_2 emissions. This efficiency is primarily attributed to hydrogen's low density, which necessitates a smaller mass per liter for storage, thus resulting in lower associated CO_2 emissions. This finding is particularly significant considering that this route's primary source of CO_2 emissions is derived from using methane in the reforming process. In contrast, the biomass-based route exhibits a reversed scenario. This process involves capturing biogenic CO_2, which leads to a carbon-negative impact. Consequently, denser storage mediums, such as ammonia or methanol, are advantageous. The higher density of these chemicals requires more biomass to produce one liter of the product, capturing a more significant amount of CO_2 and enhancing the carbon-negative effect of this route. For the electrolyzer route, methane emerges as the preferred storage medium, primarily because the CO_2 required in the methanation process is biogenic, allowing it to be considered an avoided burden and thus bringing benefits in GWP system analysis.

Fig. 4**(a)** illustrates the breakdown of GWP. In the baseline scenario A0, the GWP is primarily influenced by the reforming process, as carbon dioxide is emitted here, and using natural gas as the feedstock has a certain effect, accounting for over 80 % of the total impact. The electricity used for liquefaction contributes to the rest of GWP. When integrating a CCS unit in scenarios A1–3, there is a corresponding change in the contribution. Specifically, the contribution of the reforming process has decreased to less than 50 %. Although the use of CCS decreases carbon emissions during operation, the utilization of electricity to pressurize the inlet gas and emissions during manufacturing contribute significantly to GWP, accounting for 27.5–38.6 %. The remaining portion of GWP stems from the electricity utilized for the hydrogen storage process, including hydrogen liquefaction, PSA, and acid gas removal. For scenarios in power-based route B, the contribution to GWP follows a similar pattern, where the cell operation process contributes the most, as it consumes a significant amount of electricity compared to other processes. The highest proportion is over 90 %. Additionally, the methanation process accounts for over 20 % of the GWP because it involves carbon emissions or gas emitted during the gas-cleaning process and consumes 3.92 kWh of electricity for the production process. Hydrogen liquefaction and CCS provide another considerable amount of emission. In route C, using electricity and heat causes the pretreatment process to account for over 20 % of GWP in CL-based scenarios and around 40 % of GWP in GASF-based scenarios, respectively. For the same reason, the proportions of reforming and CL processes exceed 30 % and around 60 %, respectively.

Fig. 4**(b)** depicts the breakdown of FNEU, which is highly related to the use of electricity and heat, especially electricity. The basic trend is similar to that of GWP. The difference arises from the increasing weight of natural gas, resulting in an increment of the reforming process in route A. The breakdown of scenarios in route B remains largely consistent, with the majority of FNEU stemming from electricity consumption in the cell operation process. In route C, the proportions of bio-oil production, liquefaction, and methanation processes are larger than that in GWP, mainly due to the different influences of electricity and heat. Generating the same amount of electricity requires more fossil fuel compared to heating, increasing the contribution of those processes.

Fig. 4**(c)** illustrates the breakdown of REQD. The primary contributions stem from CCS and biomass pretreatment processes. This is due to the utilization of harmful chemicals during membrane manufacture and biomass cultivation processes, damaging the ecosystem. In route B, the membrane-based CCS process accounts for over 95 % of the total REQD, but in route C, the effect of the CCS process becomes less significant. The biomass pretreatment process predominates the REQD, which takes 90 % of REQD. Other than these two impact factors, the use of electricity and heat has a minor effect, proved by the small proportion of the cell operation process in scenarios B31-34.

Fig. 4**(d)** illustrates the breakdown of RHHD. Compared to REQD, the CCS process becomes the main contributor, followed by the biomass pretreatment process, as observed in route C. Additionally, the contribution of electricity and heat has increased. In scenarios B31-34, the percentage of the cell operation process has increased. Another piece of evidence can be found in scenarios C4-6 through the CL process, which involves a significant amount of electricity and heat. In terms of WSF, as shown in Fig. 4**(e)**, the usage of process water plays a significant role, primarily evidenced by the increasing contribution of the methanation process, accounting for up to 50 %. The cell operation process in route B and the bio-oil production process in route C also exemplify the impact of process water usage. Additionally, biomass contributes to WSF to a certain extent.

3.2. Sensitivity analysis

In the life cycle impact assessment, scenarios in the power-based route B are not entirely driven by 100% renewable energy, as the electricity used in water electrolysis is from the market. While this setup facilitates a standardized comparison across the 22 scenarios, it renders route B less competitive in terms of GWP compared to fossil fuel-based and biomass-based routes. Meanwhile, using carbon capture units and the CL process enables routes A and C to mitigate their environmental impact. The extent of the positive influence of the CCS and CL process depends on the assumed carbon capture efficiency, which is set at 90%. Both the source of electricity and carbon capture efficiency significantly influence the GWP. Therefore, a sensitivity analysis has been conducted on these two factors.

Fig. 5 illustrates the variation of GWP concerning different proportions of the renewable energy mix. A value of 0 represents 100 % solar output in the mix, while a value of 1 denotes 100 % wind output. It's worth noting that scenarios B21, B22, B23, and B24, which utilize ammonia as the storage medium, are analyzed with 100 % renewable input. The dotted lines represent the baseline in LCIA. Utilizing 100 % renewable energy results in approximately a 30 % reduction in GWP for each scenario. The average GWPs in each scenario are 0.83 kg CO_{2eq},

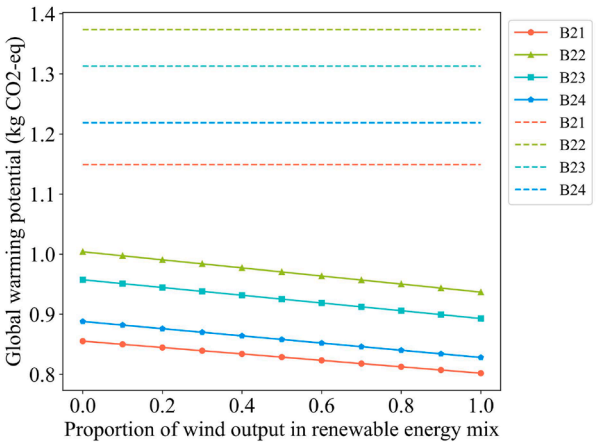

Fig. 5. The variation of GWP concerning different proportions of the renewable energy mix.

0.97 kg CO_{2eq}, 0.93 kg CO_{2eq}, and 0.86 kg CO_{2eq}, respectively. The increased utilization of wind energy will contribute to a reduction in environmental impact. In comparison to the GWP of 1.21 in scenario A2, route B becomes more competitive, but it is still higher than that in route C. However, in terms of the other four impacts, use B21 with 50% wind output in the mix as an example. FNEU and WSF are substantially reduced to 30.32 MJ and 2.44 world-eq m^3, respectively, while REQD and RHHD increase to 0.27 PDF·m^2·yr and 0.74E-6 DALY, respectively. They are less than those in route C.

Fig. 6 illustrates the variation of GWP concerning different carbon capture efficiencies. It is important to note that scenarios involving the CL process account for the emission rate of carbon dioxide, which can be used to calculate the efficiency. The sum of emission rate and efficiency is equal to 1. With changing carbon capture efficiencies, the variation of GWP in scenarios A1 and A3 is limited, ranging from 0.5 kg CO_{2eq} to 2 kg CO_{2eq}. However, the change in GWP in scenario A2 is considerable, from around 6 kg CO_{2eq} to 0.5 kg CO_{2eq}. The slope of the decline is influenced by both the amount of captured carbon dioxide and the scaling factor between the hydrogen production and storage processes. In route B, scenarios B31, B32, B33, and B34, which integrate a CCS unit, vary within the same range of 0.5 to 2. CCS is employed to provide a carbon dioxide source for methanation, with the major impact stemming from the electricity supply from the market. Therefore, the influence of capture efficiency is less significant than expected. Due to a small scaling factor of producing liquid hydrogen, scenarios C1 and C4 exhibit a flattened declining curve, whereas scenarios C2, C3, C5, and C6 demonstrate a sharp decline because of the large storage density of ammonia, methane, and methanol.

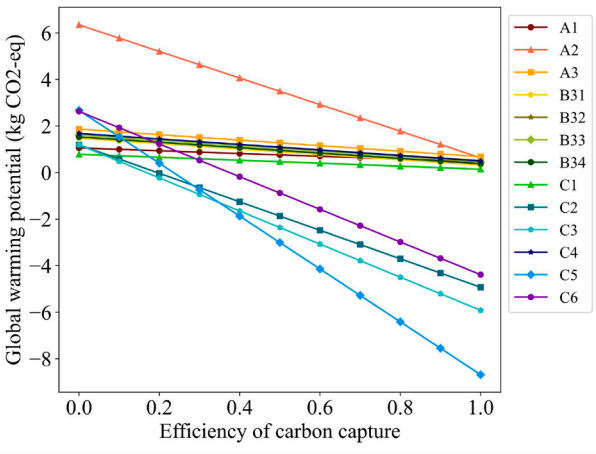

Fig. 6. The variation of GWP concerning different efficiencies of carbon capture.

4. Conclusions

This study provides a comprehensive life cycle assessment of various hydrogen production and storage routes, explicitly focusing on metrics such as carbon footprint, use of fossil and nuclear energy, ecosystem quality, human health impact, and water scarcity. In the context of the circular economy, the production of renewable synthesis fuels for energy and carbon storage based on power-to-hydrogen and biomass-to-hydrogen routes are discussed and compared with the conventional fossil fuel-based approach of steam methane reforming equipped with CCS. The conclusions are summarized as follows:

While traditional hydrogen production methods using fossil fuels are effective in certain impact categories of RHHD and WSF, they are particularly detrimental regarding CO_2 emissions. As the global push towards a net-zero emissions goal intensifies and regulations like CO_2 taxes become more stringent, integrating CCS technologies into existing systems becomes crucial. CCS can significantly mitigate emissions from traditional hydrogen production methods, serving as an effective transitional strategy, but it harms the ecosystem and human health. By aligning with circular economy principles, such as minimizing waste and reusing resources, this approach facilitates a smoother transition to future sustainable energy systems without requiring new infrastructure.

Looking ahead to a future circular economy system, converting excess renewable energy into chemical energy stands out as a strategic approach, particularly for countries with significant seasonal fluctuations in renewable electricity. This study provides a valuable guideline for such nations, advocating for implementing Power-to-X technologies to foster a more sustainable energy landscape. If a 100 % renewable electricity supply is available, the power-based route outperforms the fossil fuel-based route in terms of GWP, which is primarily influenced by electrolyzer cell operation. A higher-efficiency electrolyzer is beneficial for emission abatement.

Additionally, the LCA of biomass production routes is emphasized for their favorable outcomes due to their carbon-neutral nature. The optimal solution of using chemical looping for hydrogen production and carbon capture, as well as ammonia as the storage medium, has a negative GWP of -7.55 kg CO_{2eq}, indicating a carbon-negative system. Using gasification as the substitute is beneficial in decreasing the other four impacts and has a considerable GWP of -4.32 kg CO_{2eq}. However, the practical implementation of these findings must consider the regional availability of biomass, along with its processing and storage requirements. It is also important to note that while biomass such as wood naturally sequesters carbon, its usage can release carbon back into the atmosphere or necessitate its capture. This challenges the permanence of carbon fixation and underscores the need for careful policy and practice considerations to support sustainable and circular economic models.

Finally, this study endeavors to identify the most suitable chemical for various applications, guided by LCA perspectives. Liquid hydrogen is suitable for the fossil fuel-based route, while methane and ammonia are favorable to the power-based and biomass-based routes, respectively. The specific environmental impact category and the unique requirements of users or industrial partners determine the optimal chemical choice. Ultimately, this research underpins the critical role of informed decision-making in advancing the adoption of technologies that enhance environmental sustainability and economic viability within the circular economy framework. It is critical to highlight that the conclusions presented in this study are closely tied to the chosen functional unit and system boundaries. Should the functional unit be altered to 1 kg of hydrogen-derived product, the outcomes and interpretations might vary significantly.

CRediT authorship contribution statement

Du Wen: Writing – review & editing, Writing – original draft, Investigation, Formal analysis, Conceptualization. **Po-Chih Kuo:** Writing – review & editing, Writing – original draft, Validation, Conceptualization. **Samrand Saeidi:** Writing – review & editing, Conceptualization. **Faruk Özdemir:** Writing – review & editing, Conceptualization. **François Maréchal:** Writing – review & editing, Validation, Resources, Conceptualization.

Declaration of competing interest

The authors declare that they have no known competing financial interests or personal relationships that could have appeared to influence the work reported in this paper.

Data availability

Data will be made available on request.

Acknowledgments

The first author acknowledges the SusEcoCCUS project and the EPFL Solutions4Sustainability initiative. The authors also acknowledge the financial support of the Japan Society for the Promotion of Science under Grant No. JP-22F21041 and Ministry of National Education, Turkey.

Supplementary materials

Supplementary material associated with this article can be found, in the online version, at doi:10.1016/j.resconrec.2024.107851.

References

Aubin, P., Wang, L., Van herle, J., 2023. Evaporating water-cooled methanation reactor for solid-oxide stack-based power-to-methane systems: design, experiment and modeling. J. Chem. Eng. 456, 140256.

Bailera, M., Lisbona, P., Romeo, L.M., Espatolero, S., 2017. Power to Gas projects review: lab, pilot and demo plants for storing renewable energy and CO_2. Renew. Sustain. Energy Rev. 69, 292–312.

Batgi, S.U., Dincer, I., 2024. A study on comparative environmental impact assessment of thermochemical cycles and steam methane reforming processes for hydrogen production processes. Comput. Chem. Eng. 180, 108514.

Beckman, K., 2014. World's first power-to-liquids production plant opened in Dresden. https://energypost.eu/worlds-first-power-liquids-production-plant-opened-dresden/ (accessed June 29, 2024).

Bioenergy International, 2017. Sunfire complete industrial-scale power-to-liquid "endurance testing" https://bioenergyinternational.com/sunfire-complete-industrial-scale-power-liquid-endurance-testing/(accessed June 29, 2024).

Bioenergy International, 2020. Norsk e-Fuel reveals plans for Europe's first commercial aviation e-fuel plant. https://bioenergyinternational.com/norsk-e-fuel-reveals-plans-for-europes-first-commercial-aviation-e-fuel-plant/(accessed June 29, 2024).

Gerloff, N., 2021. Comparative Life-Cycle-Assessment analysis of three major water electrolysis technologies while applying various energy scenarios for a greener hydrogen production. J. Energy Storage 43, 102759.

Gholkar, P., Shastri, Y., Tanksale, A., 2021. Renewable hydrogen and methane production from microalgae: a techno-economic and life cycle assessment study. J. Clean. Prod. 279, 123726.

ISO, 2006a. Environmental Management-Life Cycle Assessment-Requirements and Guidelines. a.

ISO, 2006b. Environmental Management-Life Cycle Assessment-Principles and Framework. b.

Jaspers, B.C., Kuo, P.C., Amladi, A., Van Neerbos, W., Aravind, P.V., 2021. Negative CO_2 emissions for transportation. Front. Energy Res 9, 626538.

Lamers, P., Ghosh, T., Upasani, S., Sacchi, R., Daioglou, V., 2023. Daioglou. Linking Life Cycle and Integrated Assessment Modeling to Evaluate Technologies in an Evolving System Context: A Power-to-Hydrogen Case Study for the United States. Environ. Sci. Technol. 57 (6), 2464–2473.

Li, M., Middelhoff, E., Ximenes, F.A., Carney, C., Madden, B., Florin, N., Malik, A., Lenzen, M., 2022. Scenario modelling of biomass usage in the Australian electricity grid. Resour. Conserv. Recycl. 180, 106198.

Li, Y., Zhang, Z., Wang, Q., Long, X., Cao, Y., Yang, H., Yang, Q., 2023. The nitrogen and carbon footprints of ammonia synthesis in China based on life cycle assessment. J. Environ. Manag. 345, 118848.

Lindorff, M.H., 2023. The world's first dynamic, green Power-to-Ammonia plant takes shape. https://new.abb.com/news/detail/102175/the-worlds-first-dynamic-green-power-to-ammonia-plant-takes-shape (accessed June 29, 2024).

Litheko, A., Oboirien, B., Patel, B., 2023. Life cycle assessment of Power-to-Gas (PtG) technology – evaluation of system configurations of renewable hydrogen and methane production. Sustain. Energy Technol. Assessments 60, 103527.

Peters, R., Wegener, N., Samsun, R.C., Schorn, F., Riese, J., Grünewald, M., Stolten, D., 2022. A techno-economic assessment of Fischer–Tropsch fuels based on syngas from co-electrolysis. Processes 10, 699.

Prabhakaran, P., Giannopoulos, D., Köppel, W., Mukherjee, U., Remesh, G., Graf, F., Trimis, D., Kolb, T., Founti, M., 2019. Cost optimisation and life cycle analysis of SOEC based Power to Gas systems used for seasonal energy storage in decentral systems. J. Energy Storage 26, 100987.

Rolfe, A., Huang, Y., Hewitt, N., 2022. Methanol production from solid recovered fuel and lignite: techno-economic and environmental assessment. Waste Biomass Valoriz. 13, 3801–3819.

Sherrard, A., 2017. Sunfire to build 8 000 tonne-per-annum power-to-liquid facility in Norway. https://bioenergyinternational.com/sunfire-build-8-000-tonne-per-annum-power-liquid-facility-norway/(accessed June 29, 2024).

Sorrenti, I., Rasmussen, T.B.H., You, S., Wu, Q., 2022. The role of power-to-X in hybrid renewable energy systems: a comprehensive review. Renew. Sustain. Energy Rev. 165, 112380.

Sunfire, 2022. Green kerosine from 2024: norsk e-fuel presents its plans. https://www.sunfire.de/en/news/detail/green-kerosine-from-2024-norsk-e-fuel-presents-its-plans (accessed June 29, 2024).

Schropp, E., Campos-Carriedo, F., Iribarren, D., Naumann, G., Bernäcker, C., Gaderer, M., Dufour, J., 2024. Environmental and material criticality assessment of hydrogen production via anion exchange membrane electrolysis. Appl. Energy 356, 122247.

Susmozas, A., Iribarren, D., Dufour, J., 2013. Life-cycle performance of indirect biomass gasification as a green alternative to steam methane reforming for hydrogen production. Int. J. Hydrogen Energy 38, 9961–9972.

Vlap, H., van der Steen, A., Knijp, J., Holstein, J., Grond, L., 2015. Technical assumptions, technology demonstration and results P2G project.

Wang, L., Zhang, Y., Pérez-Fortes, M., Aubin, P., Lin, T.E., Yang, Y., Maréchal, F., Van herle, J., 2020. Reversible solid-oxide cell stack based power-to-x-to-power systems: comparison of thermodynamic performance. Appl. Energy 275, 115330.

Wen, D., Aziz, M., 2022. Techno-economic analyses of power-to-ammonia-to-power and biomass-to-ammonia-to-power pathways for carbon neutrality scenario. Appl. Energy 319, 119272.

Weyand, J., Habermeyer, F., Dietrich, R.U., 2023. Process design analysis of a hybrid power-and-biomass-to-liquid process – an approach combining life cycle and techno-economic assessment. Fuel 342, 127763.

Zhang, X., Bauer, C., Mutel, C.L., Volkart, K., 2017. Life Cycle Assessment of power-to-gas: approaches, system variations and their environmental implications. Appl. Energy 190, 326–338.

Zhao, G., Kraglund, M.R., Frandsen, H.L., Wulff, A.C., Jensen, S.H., Chen, M., Graves, C. R., 2020. Life cycle assessment of H_2O electrolysis technologies. Int. J. Hydrogen Energy. 45, 23765–23781.